Int J Adv Manuf Technol (2010) 51:925–933
DOI 10.1007/s00170-010-2693-4

ORIGINAL ARTICLE

Finite element modeling for maximum temperature in friction stir welding and its validation

P. Prasanna · B. Subba Rao · G. Krishna Mohana Rao

Received: 3 October 2009 / Accepted: 20 April 2010 / Published online: 19 May 2010

Abstract Friction stir welding is a relatively new joining process, which involves the joining of metals without fusion or filler materials. The amount of the heat conducted into the workpiece dictates a successful process which is defined by the quality, shape, and microstructure of the processed zone, as well as the residual stress and the distortion of the workpiece. The amount of the heat gone to the tool dictates the life of the tool and the capability of the tool to produce a good-processed zone. Hence, understanding the heat transfer aspect of the friction stir welding is extremely important, not only for the science but also for improving the process. Many research works were carried out to simulate the friction stir welding using various software to determine the temperature distribution for a given set of conditions in weldments. Very few attempted to determine the maximum temperature by varying the input parameters using ANSYS. The objective of this research is to develop a finite element simulation with improved capability to predict temperature evolution in stainless steel. The simulation model is tested with existing experimental results obtained by Zau et al. on 304 L stainless steel. The results of the simulation are in good agreement with that of experimental results. The peak temperature obtained was 1,056.853°C, which was much less than the melting point of 304 L steel (1,450°C). Error analysis is done between theoretical values for 304 L steel obtained from ANSYS and experimental values obtained by Zhu. Mean relative error is calculated between theoretical values for 304 L steel and experimental values.

Keywords Friction stir welding · Finite element modeling · ANSYS · Maximum temperature · 304 L stainless steel · Mean relative error

P. Prasanna
JNTUH College of Engg.,
Hyderabad, India

B. S. Rao
Vasavi College of Engg.,
Hyderabad, India

G. K. M. Rao (✉)
JNTUH College in Mech Engg.,
Hyderabad, India
e-mail: kmrgurram@rediffmail.com

1 Introduction to friction stir welding

Friction stir welding (FSW) is a relatively new joining process invented at The Welding Institute (Cambridge, UK) in 1991. It involves the joining of metals without fusion or filler materials. Since FSW is essentially solid state, i.e., without melting, high quality weld can generally be fabricated with absence of solidification cracking, porosity, oxidation, and other defects typical to traditional fusion welding.

Friction stir welding was used to control local properties in structural metals including aluminum and other non-ferrous and ferrous alloys. The pin may have a diameter one third of the cylindrical tool and typically has a length slightly less than the thickness of the workpiece. The pin is forced or plunged into the workpiece until the shoulder contacts the surface of the workpiece. As the tool descends further, its shoulder surface touches the top surface of the workpiece and creates heat. As the temperature of the material under the tool shoulder elevates, the strength of the material decreases.

A rotating tool with pin and shoulder is inserted in the material to be treated and traversed along the line of interest (Fig. 1). During FSW, the area to be processed and the tool

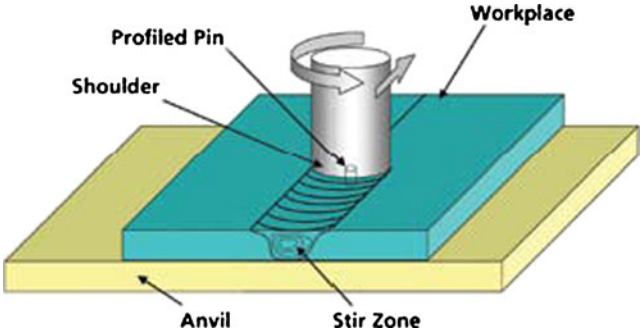

Fig. 1 Schematic of friction stir welding

are moved relative to each other such that the tool traverses with overlapping passes until the entire selected area is processed to a fine grain size. The rotating tool provides a continual hot working action, plasticizing metal within a narrow zone while transporting metal from the leading face of the pin to its trailing edge. The processed zone cools without solidification, as there is no liquid and hence a defect-free re-crystallized fine grain microstructure is formed.

The maximum temperature created by FSW process ranges from 70% to 90% of the melting temperature of the workpiece material, as measured by Tang et al. [1] and Colegrove et al. [2], so that welding defects and large distortion commonly associated with fusion welding are minimized or avoided. The heat flux in friction stir processing is primarily generated by the friction and the deformation process. This heat is conducted to both the tool and the workpiece. The amount of the heat conducted into the workpiece dictates a successful process which is defined by the quality, shape, and microstructure of the processed zone, as well as the residual stress and the distortion of the workpiece. The amount of the heat gone to the tool dictates the life of the tool and the capability of the tool to produce a good processed zone. Therefore, understanding the heat transfer aspect of the friction stir welding is extremely important, not only for the science but also for improving the process.

2 Literature survey

Friction stir welding has opened up a new process for inducing directed, localized, and controlled materials properties in any arbitrary location and pattern to achieve revolutionary capability in high value-added components. Friction stir welding provides the ability to thermo-mechanically process selective locations on the structure's surface and to some considerable depth (>25 mm) to enhance specific properties [3]. Research is being increasingly focused on this aspect of the technology for use with automotive alloys. For example, cast aluminum alloys, such as A319, are used for suspension and drive line components in automobiles.

FSW generates a fine, equiaxed grain morphology having a banded, bimodal grain size of 1-5 μm. The microstructure of friction stir welded aluminum alloy is normally stable under super plastic conditions of high temperature and dynamic strain. High-angle grain boundaries can enhance grain boundary sliding and related super plasticity [4]. However, optimum super plasticity requires a homogeneous distribution of equiaxed grains of minimum grain size. Microstructures resulting from FSW do not have a uniform grain size distribution for any one set of process parameters. Grain size varies from the top to the bottom as well as from the advancing to the retreating side. The ability of friction stir welding to change the local microstructure via thermo-mechanical working has been well established by many investigators [1].

Chao et al. investigated the variations of heat energy and temperature produced by the FSW in both the workpiece and the pin tool. All investigations showed that the FSW of Aluminum alloys yielded welds with low distortion, high quality, and low cost. Consequently, better structural performance was the primary advantage of this technology's applications [2]. In the model developed by Chao and Qi, the heat generation came from the assumption of sliding friction, where Coulomb's law was used to estimate the shear or friction force at the interface. Furthermore, the pressure at the tool interface was assumed to be constant, thereby enabling a radially dependent surface heat flux distribution as a representation of the friction heat generated by the tool shoulder, but neglecting that generated by the probe surface [5]. Frigaard et al. developed a process model for FSW, the heat input from the tool shoulder was assumed to be the frictional heat. The coefficient of friction was continuously adjusted to keep the calculated temperature from exceeding the material melting point. In principle, the FSW process could be applied to join other alloy materials such as Steels and Titanium. But, it is well known that current tool materials used in the FSW for Aluminum are not adequate for production applications in many of the harder alloy materials. However, when adequate wear resistant tool materials become available, the benefits of the FSW may promote its rapid implementation in the production of ferrous structures and structures made from other refractory materials [3, 4].

Reynolds et al. investigated the microstructures, residual stresses, and strength of the friction stir welds through experimental studies of austenitic stainless steels, and also stated that to improve the welding quality for the FSW of steels, numerical modeling, and simulations of transient temperature and residual stresses are valuable and necessary [6]. Cole grove used an advanced analytical estimation of the heat generation for tools with a threaded probe to estimate the heat generation distribution. The fraction of heat generated by the probe is estimated to be as high as

20%, which leads to the conclusion that the analytical estimated probe heat generation contribution is not negligible [7]. Song and Kovacevic investigated the influence of the preheating/dwell period on the temperature fields. They assumed a sliding condition and used an effective friction coefficient and experimental plunge force in the heat source expression [8].

Chen and Kovacevic developed a three-dimensional thermo-mechanical model including the mechanical action of the shoulder and the thermo-mechanical effect of the welded material for the FSW of an Al-alloy [9]. Schmidt et al. established an analytical model for heat generation by friction stir welding, based on different assumptions of the contact condition between the rotating tool surface and the weld piece. The material flow and heat generation were characterized by the contact conditions at the interface, and were described as sliding, sticking or partial sliding/sticking [10]. Zhu and Chao conducted three-dimensional nonlinear thermal and thermo-mechanical numerical simulations using finite element analysis code—WELDSIM on 304 L stainless steel. An inverse analysis method for thermal numerical simulation was developed [11]. McClure et al. used Rosenthal equations to calculate temperature fields in friction stir welding and found that the existence of the thermocouples and holes containing thermocouples did not influence the temperature field [12].

Ulysse used a three-dimensional visco-plastic modeling to model friction stir welding process. Forces applied on the tool were computed for various welding and rotational speeds. Pin forces increased with increasing welding speeds, but the opposite effect was observed for increasing rotational speeds [13]. Soundararajan developed a finite element thermo-mechanical model with mechanical tool loading considering a uniform value for contact conductance and used for predicting the stress at the workpiece and backing plate interface. This pressure distribution contours are used for defining the non-uniform adaptive contact conductance used in the thermal model for predicting the thermal history in the workpiece [14]. Buffa et al. developed a continuum based FEM model for friction stir welding process, which was 3D Lagrangian implicit, coupled, and rigid-viscoplastic. The distribution of temperature and strain in heat affect zone and the weld nugget was investigated. The model correctly predicted the non-symmetric nature of FSW process, and the relationships between the tool forces and the variation in the process parameters. It was found that the effective strain distribution was non-symmetric about the weld line while the temperature profile was almost symmetric in the weld zone [15].

Dickerson et al. calculated the transient heat losses into FSW tools. Heat loss into the tool enabled the welding efficiency to be determined. Finally, the use of grooves in the tool to impede heat flow was investigated as a way of increasing welding efficiency and also investigated that, using solid tools the steady state heat loss into the tool was about 10% of the total heat generated [16].

Thermal histories during FSW and their maximum values depend on the energy input from the tool, the heat loss to the backing plate and to the shank and the staying time of the tool for preheating the workpiece before it starts to move forward. It is already proved by some authors that the temperature profiles on the advancing side are slightly higher than those on the retreating side [17].

Many research works were carried out to simulate the friction stir welding using various FEA softwares to determine the temperature distribution for a given set of conditions in weldments. Very few attempted to determine the optimal temperature by varying the input parameters using ANSYS. With the emergence of faster processors and the evolution of better software, it is possible to utilize the computer's strength of rapid, linear computation on the task of building a numerical model that requires only a small amount of time and is capable of replicating experimental results from friction stir welding. Even with these improvements, a simulation still requires extensive amount of time to run till completion. Due to the FSW machineries being developed, the FSW process can be simulated through finite element softwares available.

The objective of this research is to develop a finite element simulation with improved capability to predict temperature evolution in stainless steel. The simulation model is to be tested with existing experimental results obtained by Zau et al. on 304 L stainless steel.

2.1 Finite element modeling of FSW

2.2 Introduction

The development of mathematical model for heat generation is based on the following assumptions.

1. Distribution of pressure across the interface is constant.
2. Distribution of heat across the surface of the shoulder is uniform.

The general three-dimensional partial differential equation of heat conduction in solids [14] is given by (1)

$$\frac{\partial(\rho cT)}{\partial t} = \frac{\partial}{\partial t}\left(K_x \frac{\partial T}{\partial x}\right) + \frac{\partial}{\partial t}\left(K_y \frac{\partial T}{\partial y}\right) + \frac{\partial}{\partial t} \times \left(K_z \frac{\partial T}{\partial z}\right) \quad (1)$$

where,

ρ	density, kg/mm^3
C	specific heat J/kg°C

K_x, K_y, K_z thermal conductivities along x, y, and z directions, W/m°C
T Absolute temperature, K

2.3 Heat generation

Accurate modeling of the friction stir welding process is essential to correctly represent heat generation. Modeling heat evolution between the tool and workpiece is an important step in understanding how it affects material flow and microstructure modification within and surrounding the weld.

For an ideal case, the torque required to rotate a circular shaft relative to the plate surface under the action of an axial load is given by (2)s

$$\int_0^{M_r} dM = \int_0^R \mu P(r) 2\pi r^2 dr = \frac{2}{3}\mu\pi P R^3 \tag{2}$$

where, M is the interfacial torque, μ is the friction coefficient, R is the surface radius, and P is the pressure distribution across the interface (here assumed constant).

If all the shearing work at the interface is converted into frictional heat, the average heat input per unit area and time becomes:

$$Q_1 = \int_0^{M_R} \omega dM = \int_0^R \omega 2\pi\mu \mathrm{Pr}^2 dr \tag{3}$$

where, Q_1 is the net power in watts and ω is the angular velocity in rad/s.

The next step is to express the angular velocity in terms of the rotational speed N [rotations/s]. By substituting $\omega=2\pi N$ into (3),

$$Q_1 = \int_0^R 4\pi^2 \mu PN r^2 dr = \frac{4}{3}\pi^2 \mu PN R^3 \tag{4}$$

From (4), it is obvious that the heat input depends both on rotational speed and the shoulder radius, leading to a non-uniform heat generation during welding. These parameters are the main process variables in friction stir welding, since the pressure P cannot exceed the actual flow stress of the material at the operating temperature.

In order to describe the heat source in the numerical model, it is more convenient to express the heat generation as a sum of individual contributions

$$Q_1 = \frac{4}{3}\pi^2 \mu PN \sum_{i=1}^{n} \left(R_i^3 - R_{1-1}^3\right) \tag{5}$$

where, R_{i-1} and R_i are as shown in Fig. 2.

$$\sum_{i=1}^{n} Q(R_i) = Q_1 \tag{6}$$

Hence, the energy generated from position R_{i-1} to R_i is equal to

$$\Delta Q_1 = \frac{4}{3}\pi^2 \mu PN \left(R_i^3 - R_{i-1}^3\right) \tag{7}$$

2.4 Mathematical description of moving heat source

A moving heat source with a heat distribution simulating the heat generated from the friction between the tool shoulder and the workpiece is used in the heat transfer analysis. Using an assumed friction coefficient, Frigaard et al. [4] arrived at a formula for heat generation in their modeling.

A moving cylindrical coordinate system was used for the transient movement of the heat source. Two different values of heat inputs were given to the moving heat source. Q_1 is the heat generated by the shoulder and Q_2 is the heat generated by the pin. Q_1 can be calculated by using (8)

$$Q_1 = \frac{4}{3}\pi^2 \mu PN \sum_{i=1}^{n} \left(R_i{}^3 - R_{i-1}{}^3\right) \tag{8}$$

The heat flow per unit area q_1 [8, of the shoulder can be calculated using (9)

$$q_1 = \frac{3.Q_1.r}{2\pi\left(R_s^3 - R_p^3\right)} \quad \text{for} R_s \le r \le R_p \text{ [8]} \tag{9}$$

Where

N tool rotational speed in RPM.

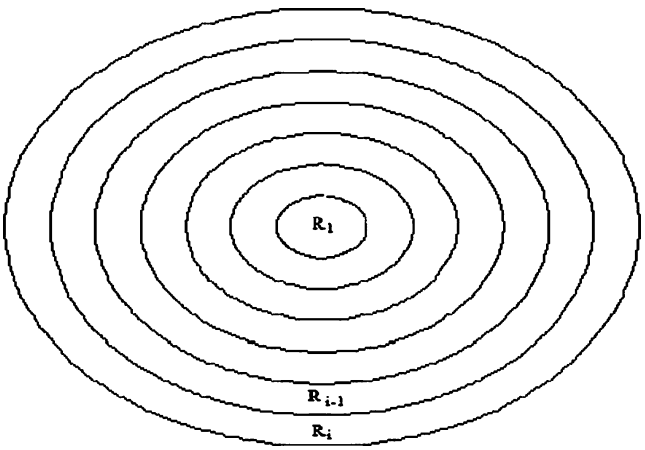

Fig. 2 Subdivision of tool shoulder into a series of volume elements of varying strengths

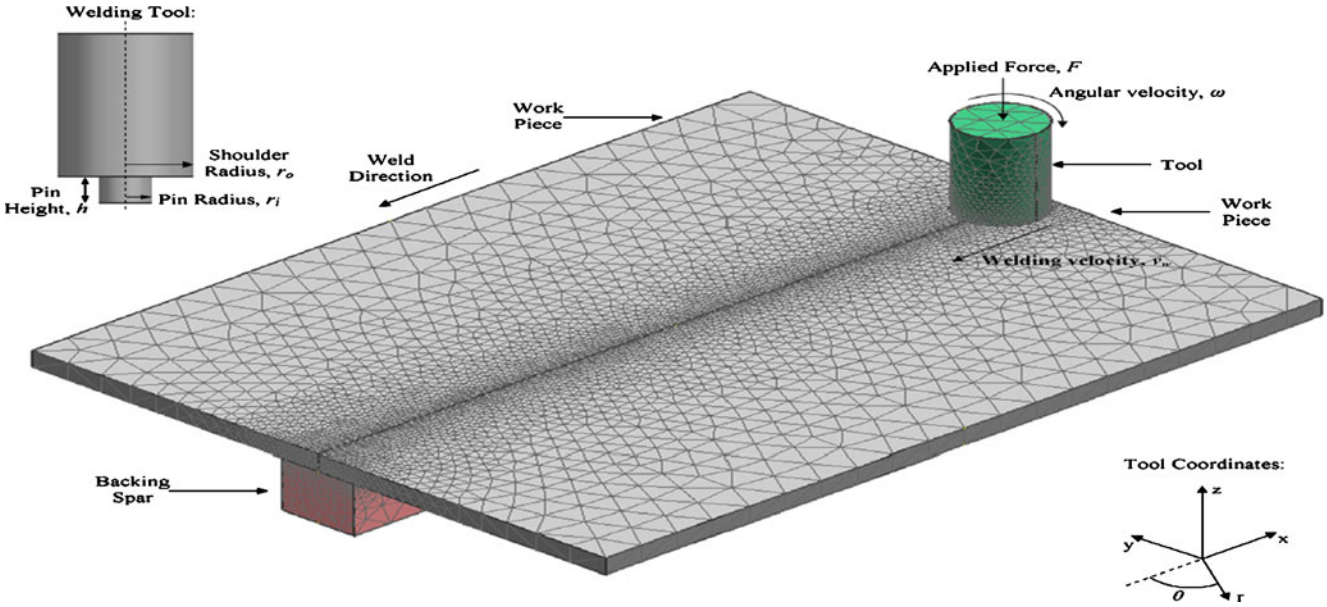

Fig. 3 Finite element model of FSW, tool coordinate system and tool geometry

P vertical force applied along the shoulder in KN
μ coefficient of friction.
R_s radius of the shoulder.
R_p radius of the tool pin.

The heat generation increases as the distance from the center increases. However, for simplicity, a uniform distribution of heat across the surface of the shoulder is assumed. Hence, for uniform distribution, the average value of radius of tool shoulder and tool pin was taken,

$$r = \frac{R_s + R_p}{2} \tag{10}$$

2.5 Heat generation from the pin

From Schmidt et al. [10], the ratio of heat generated from the pin Q_2, and the heat generated from the shoulder Q_1, was 0.128. Hence heat flow per unit area of the pin q_2 is also 0.128 times q_1.

This q_1 and q_2 were given as inputs to the finite element model for simulation purpose.

2.6 Boundary conditions

The boundary and initial conditions that are applied to the heat transfer model [10] shown in Fig. 3 are given as follows:

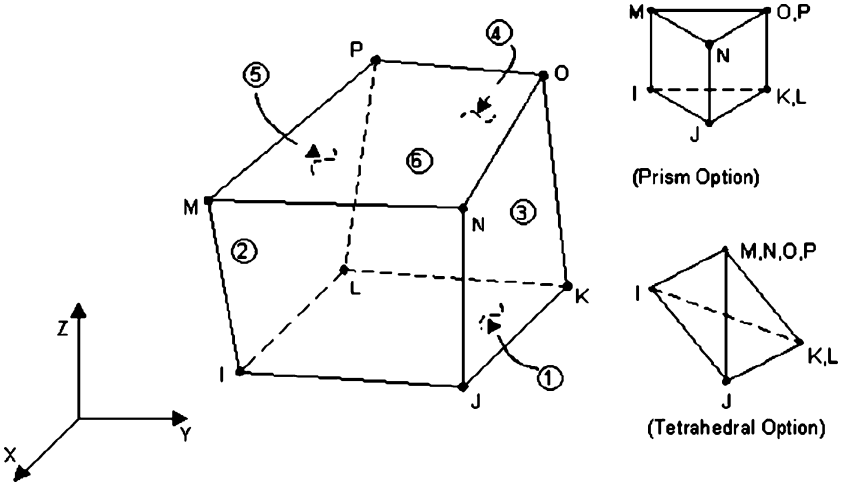

Fig. 4 Solid-70 element

Table 1 Temperature dependent material properties for 304 L steel

Sl. No	Temperature (°C)	Thermal conductivity (W/m°C)	Specific heat (J/Kg° C)	Enthalpy (J/kg)
1	0	16	500	0.1365e06
2	200	19	540	0.25542e06
3	400	21	560	0.37688e06
4	600	24	590	0.51507e06
5	800	29	600	0.6438e06
6	1,000	30	610	0.77653e06

The initial boundary condition for the calculation is

$$T(x,y,z,t) = T_0 \tag{11}$$

The heat flux boundary condition at the tool and workpiece interface is given by

$$k.\frac{\partial T}{\partial n} = q \tag{12}$$

The convective boundary condition for all the workpiece surfaces exposed to the air is

$$k.\frac{\partial T}{\partial n} = h(T - T_0) \tag{13}$$

where n is the normal direction vector of the boundary.

From (12) and (13) the convection coefficient can be given as $q = h(T - T_0)$

The two plates that were to be welded are assumed identical. At the centerline of the workpiece, the temperature gradient in the transverse direction equals to zero due to the symmetrical requirement.

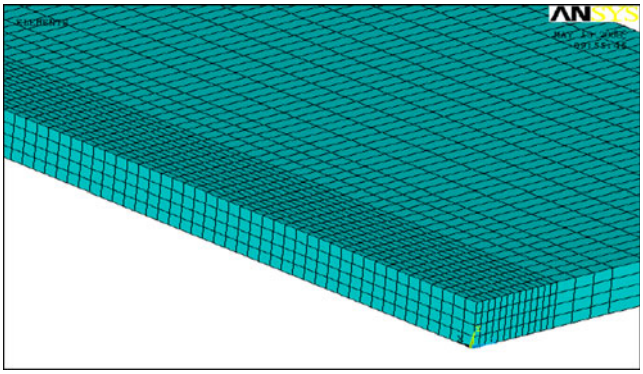

Fig. 5 Meshed model of the workpiece (*isometric view*)

2.7 Material properties

Thermal conductivity, K and heat capacity, C are dependent on temperature. The ambient temperature was assumed to be 25°C. The initial temperature of the workpiece is assumed to be equal to the ambient temperature. The origin (0,0,0) is considered to be at the intersection of the center line (process line) and the edge line on the top surface where FSW begins.

As the temperature increases, the material softens and the value of friction coefficient drops down. A major problem in modeling of heat flow phenomena in friction stir processing is to obtain an adequate description of the energy input. This is because the friction coefficient, μ, was changing continuously during welding from about one at

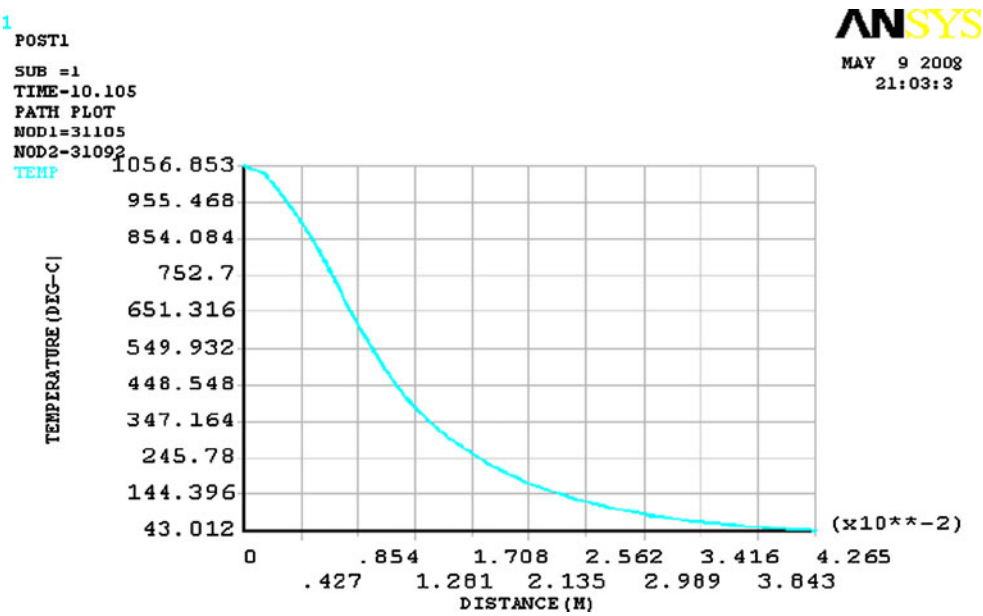

Fig. 6 Temperature distributions on top surface

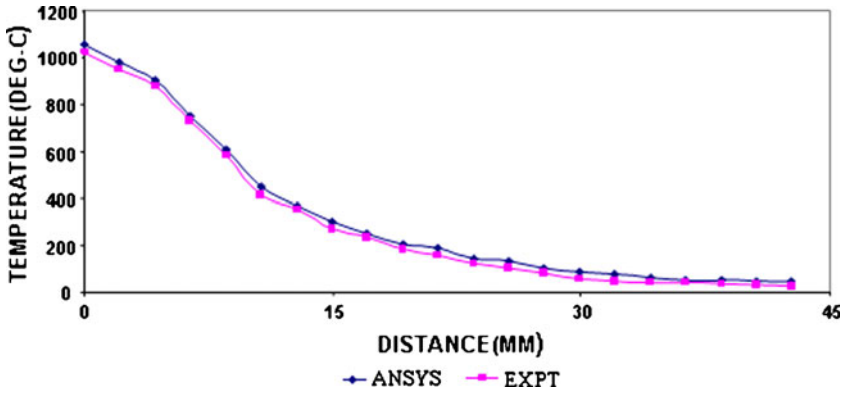

Fig. 7 Variation in temperature with distance perpendicular to the weld line

the dry sliding start, towards zero when the temperature for local melting is reached at the interface.

2.8 Element selection

SOLID70 which is a three-dimensional thermal solid, is used as the element type for analysis. SOLID70 has a three-dimensional thermal conduction capability. The element has eight nodes with a single degree of freedom, temperature, at each node. The element is applicable to a three-dimensional, steady-state, or transient thermal analysis. The element also can compensate for mass transport heat flow from a constant velocity field. If the model containing the conducting solid element is also to be analyzed structurally, the element should be replaced by an equivalent structural element such as SOLID45.

The element shown in Fig. 4 is defined by eight nodes and the orthotropic material properties. Orthotropic material directions correspond to the element coordinate directions. Specific heat and density are ignored for steady state solutions. Convection or heat flux and radiation may be input as surface loads at the element faces as shown by the circled numbers in Fig. 4. Heat generation rates may be input as element body loads at the nodes. Convection heat flux was positive out of the element; applied heat flux is positive into the element.

2.9 Contact condition

When modeling the FSW process, the contact condition is the most critical part of the numerical model. Contact condition can be classified into three categories. They are explained in the following paragraphs.

Sticking condition If the friction shear stress exceeds the yield shear stress of the underlying matrix then the matrix surface will stick to the moving tool surface segment. In this case, the matrix segment will accelerate along the tool surface (finally receiving the tool velocity), until equilibrium state is established between the contact shear stress and the internal matrix shear stress. At this point, the stationary full sticking condition is fulfilled. In conventional Coulomb's friction law terms, the static friction coefficient relates the reactive stresses between the surfaces.

Sliding condition If the contact shear-stress is smaller than the internal matrix yield shear-stress, the matrix segment volume shears slightly to a stationary elastic deformation, where the shear stress equals the 'dynamic' contact shear stress. This state is referred to as the sliding condition.

Partial sliding/sticking The last possible state between the sticking and sliding condition is a mixed state of the two. In this case, the matrix segment accelerates to a velocity less than the tool surface velocity, where it stabilizes. The equilibrium establishes when the 'dynamic' contact shear stress equals the internal yield shear stress due to a quasi-stationary plastic deformation rate. This is referred to as the

Table 2 Error analysis of 304 L steel

SI. No	Distance (mm)	Theoretical temperature (°C) (APDL)	Experimental temperature (°C) ZUE	M.R.E (%)
1	3	955.143	941	1.48
2	6	752.306	736	2.166
3	9	560.107	546	2.5
4	12	400.216	376	6.0
5	15	282.127	261	7.48
6	18	230.187	216	6.16
7	21	180.206	163	9.54
8	24	130.406	112	14.14
9	27	115.183	98	14.91
10	30	100.143	86	14.12
11	33	80.646	63	21.88
12	36	60.549	48	20.72
13	39	50.636	40	21.00
14	42	40.136	32	20.27

MRE mean relative error

partial sliding/sticking condition. In this model, there is no difference between the dynamic and the static friction coefficients.

3 Results and discussion

Friction stir welding of material 304 L stainless steel was simulated and compared with the experimental results of Zhu et al. [8]. To maintain consistency, the dimensions of the workpiece, material properties, radius of the shoulder and pin, length of the pin, rotational speed, and welding speed used were considered same as Zhu et al. The workpiece had dimensions of 304.8×203.2×3.2 mm^3, the tool had a shoulder radius of 9.25 mm, pin radius of 6.32 mm and pin length of 2.9 mm. A rotational speed of 300 rpm and a welding speed of 1.69 mm/s were used for carrying out the simulation. The tool penetrates at a point which is 6.44 mm away from the edge of the workpiece. The material properties of 304 L stainless steel are given in Table 1. The density of 304 L stainless steel is 7.45 E-06 Kg/mm^3.

Figure 5 shows a meshed model for 304 L steel material. A moving cylindrical coordinate system as, shown in Fig. 5, was used to move the heat source. Instead of moving the heat source continuously, it was moved in steps, so the heat was applied at each successive point one after the other chronologically. By making the distance between successive points very small, a close approximation to the continuous movement could be achieved.

It is assumed that two plates were square butt welded. As the weld line was the symmetrical line, only one half of the workpiece 304.8×203.2×3.2 was modeled using commercial finite element package ANSYS (APDL). At all the surfaces except at the bottom a convective heat transfer of 30 W/m^2 °C was used for natural convection between 304 L and air. In friction stir welding, the workpieces were clamped over back plates and clamped. A higher convective coefficient of 350 W/m^2 °C is applied as a boundary condition to the bottom surface of the workpiece.

The coordinate system was moved after each load step. At every load step a set of elements in the shape of the tool are selected and heat flux was applied on the surfaces of the elements. A time step of 0.09 s was used. APDL (ANSYS parametric design language) was used to write a subroutine for a looping transient moving heat source model.

Figure 6 shows the temperature distribution on the top surface, perpendicular to welding direction. Figure 7 shows the results obtained from FEA and by Zhu et al. The results of the simulation are in good agreement with that of experimental results. The peak temperature obtained was 1,056.853°C, which was much less than the melting point of 304 L steel (1,450°C).

4 Error analysis between theoretical values for 304 L steel and experiments conducted by Zhu

Error analysis is done between theoretical values for 304 L steel obtained from ANSYS and experimental values obtained by Zhu. Mean relative error is calculated between theoretical values for 304 L steel and experimental values and are shown in Table 2.

5 Conclusion

A finite element simulation model is developed with improved capability to predict peak temperature during friction stir welding of 304 L steel and this model is validated with existing experimental results of Zau et al. Mean error analysis is performed between experimental results and results obtained from simulated model.

References

1. Colegrove P, Painter M, Graham D, Miller T (2000) 3-Dimensional flow and thermal modeling of the friction stir welding process. Proceedings of the Second International Symposium on Friction Stir Welding, June 26–28, Gothenburg, Sweden
2. Chao YJ, Qi X, Tang W (2003) Heat transfer in friction stir welding—experimental and numerical studies. ASME J Manuf Sci Eng 25:138–145
3. Frigaard G, Midling OT (1998) Modeling of the heat flow phenomena in friction stir welding of aluminum alloys. Proceedings of the Seventh International Conference Joints in Aluminum —INALCO '98, Cambridge, UK, April 15-17, pp 1189-1200
4. Frigaard G, Midling OT (2001) A process model for friction stir welding of age hardening aluminum alloys. Metallurgical and Materials Transactions A, Physical Metallurgy and Materials Science 32A (5) May 2001, ASM International, pp. 1189-2000. 32A
5. Chao YJ, Qi X (1998) Thermal and thermomechanical analysis of friction stir joining of AA6061-T6. J Mater Process Manuf Sci 7:215–233
6. Reynolds AP, Lockwood WD, Seidel TU (2000) Processing–property correlation in friction stir welds. Mater Sci Forum 331–337:1719–1724
7. Colegrove PA, Shercliff HR (2003) Experimental and numerical analysis of aluminium alloy 7075-T7351 friction stir welds. Sci Tech Weld Join 8(5). IoM Communications Ltd, pp 360-368
8. Song M, Kovacevic R. Numerical and experimental study of the heat transfer process in friction stir welding. Proc Inst Mech Eng USA 217 Part B: J Eng Manuf
9. Chen CM, Kovacevic R (2003) Finite element modeling of friction stir welding—thermal and thermo-mechanical analysis. Int J Mach Tools Manuf 43:1319–1326
10. Schmidt H, Hattel J, Wert J (2004) An analytical model for the heat generation in friction stir welding. Model Simul Mater Sci Eng 12:143–157
11. Zhu XK, Chao YJ (2004) Numerical simulation of transient temperature and residual stresses in friction stir welding of

304 L stainless steel. J Mater Process Technol 146:263–272
12. McClure JC, Tang W, Murr LE, Guo X, Feng Z, Gould JE (1998) A thermal model of friction stir welding. International Conference on Trends in Welding Research 349:156–165
13. Ulysse P (2002) Three dimensional modeling of friction stir welding process. Int J Mach Tools Manuf 42:1549–1557
14. Soundararajan V, Zekovic S, Kovacevic R (2005) Thermo-mechanical model with adaptive boundary conditions for friction stir welding of Al 6061. Int J Mach Tools Manuf 45:1577–1587
15. Buffa G, Huaa J, Shivpuri R, Fratini L (2006) A continuum based fem model for friction stir welding—model development. J Mater Sci Eng A419:389–396
16. Dickerson T, Shi Q-Y, Shercliff HR (2003) Heat flow into friction stir welding tools. Proceedings of 4th international symposium on friction sitr welding, USA, pp 14-16
17. Hwang Y-M, Kang Z-W, Chiou Y-C, Hsu H-H (2008) Experimental study on temperature distributions within the workpiece during friction stir welding of aluminium alloy. Int J Mach Tools Manuf 48:778–787